PHYSICAL REVIEW C **80**, 052201(R) (2009)

Backward-angle η photoproduction from protons at $E_\gamma = 1.6$–2.4 GeV

M. Sumihama,[1] D. S. Ahn,[1,2] J. K. Ahn,[2] H. Akimune,[3] Y. Asano,[4] W. C. Chang,[5] S. Daté,[4] H. Ejiri,[1] H. Fujimura,[6] M. Fujiwara,[1] S. Fukui,[7] S. Hasegawa,[8] K. Hicks,[9] T. Hotta,[1] K. Imai,[10] T. Ishikawa,[6] T. Iwata,[11] Y. Kato,[1] H. Kawai,[12] K. Kino,[13] H. Kohri,[1] N. Kumagai,[14] T. Matsuda,[15] T. Matsumura,[16] T. Mibe,[17] M. Miyabe,[1] N. Muramatsu,[1] T. Nakano,[1] M. Niiyama,[18] M. Nomachi,[19] Y. Ohashi,[4] H. Ohkuma,[4] T. Ooba,[12] D. S. Oshuev,[5] C. Rangacharyulu,[20] A. Sakaguchi,[19] P. M. Shagin,[21] Y. Shiino,[12] A. Shimizu,[1] H. Shimizu,[6] Y. Sugaya,[19] Y. Toi,[15] H. Toyokawa,[4] A. Wakai,[22] C. W. Wang,[5] S. C. Wang,[5] K. Yonehara,[23] T. Yorita,[1] M. Yoshimura,[24] M. Yosoi,[1] and R. G. T. Zegers[25]

(LEPS Collaboration)

[1]*Research Center for Nuclear Physics, Osaka University, Ibaraki, Osaka 567-0047, Japan*

[2]*Department of Physics, Pusan National University, Busan 609-735, Korea*

[3]*Department of Physics, Konan University, Kobe, Hyogo 658-8501, Japan*

[4]*Japan Synchrotron Radiation Research Institute, Sayo, Hyogo 679-5198, Japan*

[5]*Institute of Physics, Academia Sinica, Taipei 11529, Taiwan*

[6]*Laboratory of Nuclear Science, Tohoku University, Sendai, Miyagi 982-0826, Japan*

[7]*Department of Physics and Astrophysics, Nagoya University, Aichi 464-8602, Japan*

[8]*J-PARC Center, Japan Atomic Energy Agency, Tokai-mura, Ibaraki 319-1195, Japan*

[9]*Department of Physics and Astronomy, Ohio University, Athens, Ohio 45701, USA*

[10]*Department of Physics, Kyoto University, Kyoto 606-8502, Japan*

[11]*Department of Physics, Yamagata University, Yamagata 990-8560, Japan*

[12]*Department of Physics, Chiba University, Chiba 263-8522, Japan*

[13]*Graduate School of Engineering, Hokkaido University, Sapporo, Hokkaido 060-8628, Japan*

[14]*XFEL Project Head Office, RIKEN, Sayo, Hyogo 679-5198, Japan*

[15]*Department of Applied Physics, Miyazaki University, Miyazaki 889-2192, Japan*

[16]*National Defense Academy in Japan, Yokosuka, Kanagawa 239-8686, Japan*

[17]*High Energy Accelerator Research Organization, KEK, Tsukuba, Ibaraki 305-0801, Japan*

[18]*RIKEN, The Institute of Physical and Chemical Research, Wako, Saitama 351-0198, Japan*

[19]*Department of Physics, Osaka University, Toyonaka, Osaka 560-0043, Japan*

[20]*Department of Physics and Engineering Physics, University of Saskatchewan, Saskatoon, Saskatchewan S7N 5E2, Canada*

[21]*School of Physics and Astronomy, University of Minnesota, Minneapolis, Minnesota 55455, USA*

[22]*Akita Research Institute of Brain and Blood Vessels, Akita 010-0874, Japan*

[23]*Illinois Institute of Technology, Chicago, Illinois 60616, USA*

[24]*Institute for Protein Research, Osaka University, Suita, Osaka 565-0871, Japan*

[25]*National Superconducting Cyclotron Laboratory, Michigan State University, Michigan 48824-1321, USA*

(Received 25 September 2009; published 30 November 2009)

Differential cross sections for η photoproduction from protons have been measured at $E_\gamma = 1.6$–2.4 GeV in the backward direction. A bump structure has been observed above 2.0 GeV in the total energy. No such bump is observed in η', ω, and π^0 photoproductions. It is inferred that this unique structure in η photoproduction is due to a baryon resonance with a large $s\bar{s}$ component that is strongly coupled to the ηN channel.

DOI: 10.1103/PhysRevC.80.052201 PACS number(s): 13.60.Le, 14.20.Gk, 25.20.Lj

The constituent quark model has been very successful in describing the ground state of the flavor SU(3) octet and decuplet baryons. Many baryon resonances predicted by the constituent quark model have been discovered and are well established [1–3]. There are two well-known problems for the three-quark model of baryons. One is the mass-order-reverse problem for the lowest excited state [4]. According to the constituent quark model, the negative-parity state with the orbital angular momentum $L = 1$ should be the lowest except for protons and neutrons. However, the lowest has been experimentally found as $S_{11}(1535)$, which is heavier than $P_{11}(1440)$ and $\Lambda(1405)$ with an s quark. This mass-order-reverse problem may be solved by taking into account the extra quark and antiquark pair. A large admixture of $s\bar{s}$ for $S_{11}(1535)$, $u\bar{u}$ for $P_{11}(1440)$, and $d\bar{d}$ for $\Lambda(1405)$ was proposed to explain the mass order of these resonances [4]. As a natural consequence of a large $s\bar{s}$ admixture in $S_{11}(1535)$, we expect a strong coupling to ηN because the η meson is the lightest meson with an $s\bar{s}$ component.

The other problem is concerned with so-called "missing baryon resonances." Many resonances around 2 GeV are predicted in the constituent quark model. However, a large number of them are not identified experimentally. Information on baryon resonances comes mainly from the pion induced productions. Some missing resonances may couple to other mesons such as ηN, ωN, and $K\Lambda$ and could escape search [3]. The study of η photoproduction has the advantage of looking for specific resonances with large $s\bar{s}$ components and an isospins of $\frac{1}{2}$ by means of decay into ηN.

Recently, η photoproduction has been studied by the CB-ELSA and CLAS collaborations. An enhancement of differential cross sections was observed around $W = 1.85$ GeV in the total energy and was claimed by CLAS [5] to be attributable to the third S_{11} resonance. However, CB-ELSA found evidence of a new resonance $D_{15}(2070)$, but did not observe the third S_{11} resonance [6]. The BES collaboration found a peak around 2065 MeV in the invariant mass spectrum of πN from J/ψ decay into $\bar{N}N\pi$ [7]. The peak is suggested to be attributable to the $P_{11}(2100)$ resonance, which is predicted by the Pitt-ANL model [1,8] to couple strongly to ηN. The πN system in this decay mode has an isospin of $\frac{1}{2}$. All the experimental results indicate that there are some unestablished resonances around 2 GeV. Therefore, it is expected that the additional precise measurement of η photoproduction will shed light on the nature of these resonances.

In this article, we report the differential cross sections of backward-angle η photoproductions from protons in the energy range $E_\gamma = 1.6$–2.4 GeV by detecting protons at forward angles to identify η mesons in the missing-mass spectrum. At backward angles, no appreciable contribution is expected from forward diffractive processes, and it is expected that one can clearly observe resonances.

The experiment was carried out at the SPring-8/LEPS facility [9]. The laser-electron photon beam was produced by backward-Compton scattering between Ar-ion laser photons with a 351-nm wavelength and electrons with 8-GeV energy. The photon energy range was 1.6–2.4 GeV. The energy resolution was 10 MeV in root-mean-square. A liquid hydrogen target with a thickness of 16.5 cm was used. The data were accumulated with 1.0×10^{12} photons at the target. Charged particles were detected by using the LEPS magnetic spectrometer. The angular coverage of the spectrometer was about $\pm 20^\circ$ and $\pm 10^\circ$ in the horizontal and vertical directions, respectively. Charged-particle events with confidence levels of a track fitting of greater than 98% were used in this analysis. Mass identification was made using momentum, path length, and time of flight. The momentum range of protons was 1.4–2.4 GeV/c in the present analysis. The momentum resolution for 1.4 to 2.4 GeV/c protons was 0.7%–0.9%. The proton mass resolution was 46 MeV/c^2 at 2 GeV/c momentum. Proton events were selected in the reconstructed mass spectrum within 4σ of the nominal value [10]. Contaminations from pions and kaons were estimated to be less than 0.1%. Reaction vertex points were reconstructed as the closest point between a track and the beam axis and were used to select events produced from the liquid hydrogen target. Some contaminations came from the events produced in a charge-defining plastic scintillator placed behind the target. The contamination rate was typically 1% but increased up to 5% at a scattering angle less than 6° because of poorer vertex reconstruction resolution. The spectrometer acceptance, including the efficiency for detectors and track reconstruction, was obtained using a Monte Carlo simulation with the GEANT3 code [11]. The acceptance, which depended on the photon energy and the scattering angle, was calculated. Detailed descriptions about the detectors and particle identification are given in Refs. [9,10].

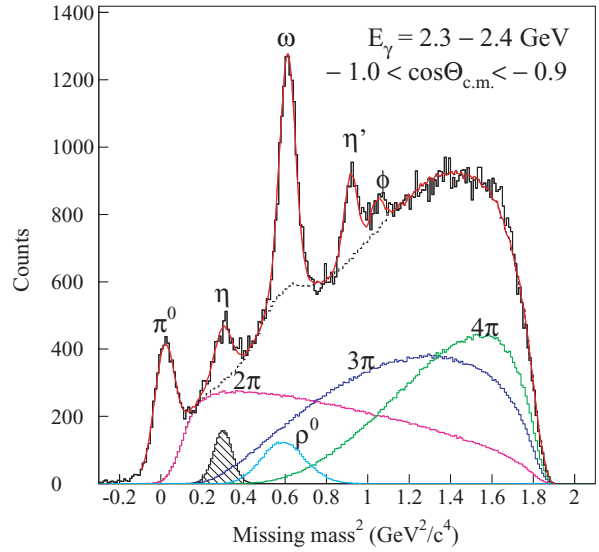

FIG. 1. (Color online) Spectrum of missing mass square for $\gamma p \to pX$ at $E_\gamma = 2.3$–2.4 GeV and $\cos\Theta_{\mathrm{c.m.}} = -1.0$ to -0.9, where $\Theta_{\mathrm{c.m.}}$ is the scattering angle of mesons. The peaks are attributable to π^0, η, ω, η', and ϕ meson photoproductions. The red curve is the fitting results. The pink, blue, green, and light-blue curves are for 2π, 3π, 4π, and ρ^0 photoproductions determined by a fit to the data, respectively. The dashed curve is the distribution of the sum of them. The hatched histogram is for the η meson.

The data were divided into eight energy bins from 1.6 to 2.4 GeV, and four angular bins from -1.0 to -0.6 in $\cos\Theta_{\mathrm{c.m.}}$, where $\Theta_{\mathrm{c.m.}}$ is the scattering angle of mesons in the center-of-mass system. The spectrum of missing mass square for the $\gamma p \to pX$ reaction is shown in Fig. 1. The peaks observed are due to π^0, η, ω, η', and ϕ meson photoproductions. The background under the η meson peak consists of nonresonant 2π, 3π, and ρ^0 photoproductions. The missing mass distributions for each photoproduction at different energies and at different angular bins were generated in the Monte Carlo simulation by taking into account the detector resolution of the present experiment. The experimental data were fitted by summing all the generated missing-mass distributions of signal and background processes. The contribution of each reaction channel was determined by the relative height of the distribution to minimize the fitting χ^2. The reduced χ^2 was 1.2 at minimum and 2.3 at maximum, depending on the angular and energy binning. The contributions of each reaction channel in the fitting are shown in Fig. 1. Finally, the yield of η was extracted from the fit. The energy dependence of cross sections for the nonresonant multipion productions was estimated from the fitting and assumed to be smooth in determining the generated distributions. The distribution for 2π production, which is the main background for η photoproduction, gradually decreases toward high energies.

Experimentally, the statistics of η photoproduction increased with the scattering angles of η meson and with energies because the spectrometer acceptance was larger at smaller angles of protons and the number of photons is larger at higher energies. The statistical error is 4% at minimum at $W = 2.20$–2.24 GeV and at $-1.0 < \cos\Theta_{\mathrm{c.m.}} < -0.9$ and

is 13% at maximum at $W = 1.97$–2.02 GeV and at $-0.7 < \cos\Theta_{\text{c.m.}} < -0.6$. Background events from the charge-defining plastic scintillator behind the target make a broad missing mass distribution attributable to the Fermi motion. The contamination rate was estimated to be 3% and 0.5% at $-1.0 < \cos\Theta_{\text{c.m.}} < -0.9$ and $-0.9 < \cos\Theta_{\text{c.m.}} < -0.6$, respectively, and was subtracted from the yields.

The systematic uncertainty for the resolution estimated in Monte Carlo simulation is obtained from the η peak fitting by using the Gaussian function. The systematic uncertainty is 4% at minimum and 20% at maximum. The systematic uncertainty obtained for the background subtraction due to the uncertainty of the energy dependence was 0.1%–3.3%. The systematic uncertainty for the target thickness, attributable to fluctuations of the temperature and pressure of the liquid hydrogen, was estimated to be 1.0%. The systematic error of the photon number normalization was 3.0%. The systematic uncertainty of the aerogel Čerenkov counter attributable to accidental vetoes and δ rays was measured to be lower than 1.6%. The overall systematic uncertainties were calculated as the square root of the quadratic sum of these systematic uncertainties and were 3.6%–20.1%.

Figure 2 shows the differential cross sections for η photoproduction. The differential cross sections have been obtained for the first time in the angular range of $-1 < \cos\Theta_{\text{c.m.}} < -0.8$. A wide bump structure has been observed above 2.0 GeV in the total energy W. The present results are consistent with the data from CLAS and CB-ELSA that indicate the presence of a bump structure around $W = 2.1$ GeV.

The maximum cross section of the bump amounts to about 0.08 μb/sr on top of the continuum background, which may come from the nonresonant process. The background decreases with increasing energy (shown by the solid curves in Fig. 2). Therefore, the bump is comparable to the background. To explain the presence of a large bump, a contribution from resonances is required. The central position of the bump structure shifts to higher energies at backward angles. The locations are $W \sim 2.06$ GeV at $-0.7 < \cos\Theta_{\text{c.m.}} < -0.6$ and $W \sim 2.17$ GeV at $-1.0 < \cos\Theta_{\text{c.m.}} < -0.9$. This is possible because an interference between resonances and diffractive processes may depend on the scattering angles. The other possibility is that the bump structure consists of more than one resonance whose angular distributions are different.

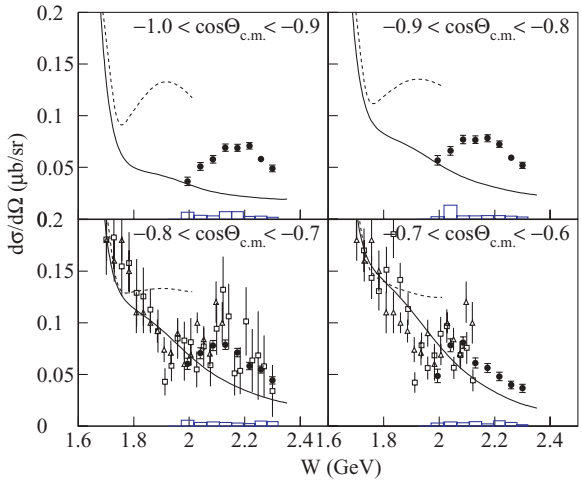

FIG. 2. (Color online) Differential cross sections for η photoproduction plotted as a function of the total energy W. The angular range is indicated. The solid circles are the present results. Statistical error is plotted as error bars, and the blue boxes show systematic uncertainties. The open triangles and open squares are the experimental data from CLAS [5] and CB-ELSA [6], respectively. The solid and dashed curves are the results of SAID [12] and ETA-MAID [13], respectively.

The SAID calculations are consistent with the experimental data below 2.0 GeV but underestimate the data above 2 GeV. An additional process is needed for explaining the bump structure above 2 GeV. In the SAID analysis, the possible resonance is $G_{17}(2190)$ with $(M,\ \Gamma) = (2152, 484)$ MeV around 2.1 GeV [14]. The results of ETA-MAID are consistent with the data below 1.8 GeV. However, the bump structure does not appear in the calculation [13]. Although the central position of the bump structure in the present analysis moves from 2.06 to 2.17 GeV, the position and the bump width is roughly consistent with those of the resonance D_{15} with $(M,\ \Gamma) = (2068$ MeV, 295 MeV) as suggested by the CB-ELSA collaboration work [6]. Detailed studies including the precise angular distribution at backward angles will help to improve theoretical calculations by revealing the hidden resonance states contributing to the bump structure.

Figure 3 shows the differential cross sections for η, η', ω, and π^0 photoproductions. Differential cross sections for η', ω, and π^0 photoproductions have been simultaneously obtained in the present analysis. The results on π^0 photoproduction have been reported in Ref. [10]. A small bump structure is observed around 2.25 GeV in η' photoproduction. There is no prominent structure for the ω photoproduction cross section. The cross section for π^0 photoproduction drastically decreases with energies up to 2.15 GeV and shows a mostly

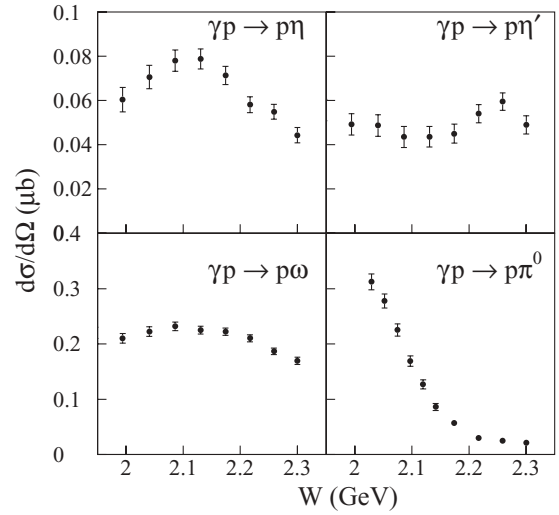

FIG. 3. Differential cross sections for η, η', ω, and π^0 photoproductions plotted as a function of the total energy W at $-0.8 < \cos\Theta_{\text{c.m.}} < -0.7$.

flat distribution above 2.15 GeV. The energy dependencies of cross sections for π^0, η', and ω photoproductions are different from that for η photoproduction. The wide bump structure is a specific character of η photoproduction. Therefore, the bump structure is expected to be attributable to resonances with a large $s\bar{s}$ component and with a strong coupling to the ηN channel.

In summary, η photoproduction from protons has been measured at $E_\gamma = 1.6$–2.4 GeV at the SPring-8/LEPS facility. The differential cross sections have been obtained with high statistics at backward scattering angles of η mesons in the $\gamma p \to p\eta$ reaction by detecting protons scattered at forward angles. This work provides unambiguous evidence of a bump structure above $W = 2.0$ GeV. No such structure is seen in η', ω, and π^0 photoproductions. It is inferred that this unique structure in η photoproduction is attributable to a baryon resonance with a large $s\bar{s}$ component that coupled strongly to the ηN channel.

We thank the staff at SPring-8 for providing excellent experimental conditions. We thank I. I. Strakovsky for fruitful discussions on the possible resonances around 2.1 GeV. This work was supported in part by the Ministry of Education, Science, Sports and Culture of Japan; the National Science Council of the Republic of China (Taiwan); the National Science Foundation (USA); and the Yamada Science Foundation.

[1] Particle Data Group, Phys. Lett. **B667**, 1 (2008).
[2] N. Isgur and G. Karl, Phys. Rev. D **18**, 4187 (1978); **19**, 2653 (1979).
[3] S. Capstick and W. Roberts, Phys. Rev. D **49**, 4570 (1994); **58**, 074011 (1998); S. Capstick and W. Roberts, Prog. Part. Nucl. Phys. **45**, S241 (2000).
[4] B. S. Zou, Nucl. Phys. **A790**, 110c (2007).
[5] M. Dugger *et al.* (CLAS Collaboration), Phys. Rev. Lett. **89**, 222002 (2002).
[6] V. Crede *et al.* (CB–ELSA Collaboration), Phys. Rev. Lett. **94**, 012004 (2005).
[7] M. Ablikim *et al.* (BES Collaboration), Phys. Rev. Lett. **97**, 062001 (2006).
[8] T. P. Vrana, S. A. Dytman, and T.-S. H. Lee, Phys. Rep. **328**, 181 (2000).
[9] M. Sumihama *et al.* (LEPS Collaboration), Phys. Rev. C **73**, 035214 (2006); T. Nakano *et al.* (LEPS Collaboration), *ibid.* **79**, 025210 (2009).
[10] M. Sumihama *et al.* (LEPS Collaboration), Phys. Lett. **B657**, 32 (2007).
[11] R. Brun *et al.*, Applications Software Group, CERN Program Library Long Writeup W5013.
[12] R. A. Arndt, W. J. Briscoe, I. I. Strakovsky, and R. L. Workman, Phys. Rev. C **74**, 045205 (2006); http://gwdac.phys.gwu.edu/.
[13] L. Tiator and S. Kamalov, Maid Analysis Techniques, arXiv:nucl-th/0603012; D. Drechsel, O. Hanstein, S. S. Kamalov, and L. Tiator, Nucl. Phys. **A645**, 145 (1999); http://www.kph.uni-mainz.de/MAID/.
[14] I. I. Strakovsky (private communication).